Journal of Zhejiang University-SCIENCE B (Biomedicine & Biotechnology) 2025 26(2):124-144
www.jzus.zju.edu.cn; www.springer.com/journal/11585
E-mail: jzus_b@zju.edu.cn

Review

https://doi.org/10.1631/jzus.B2300614

Advancements in molecular imaging probes for precision diagnosis and treatment of prostate cancer

Jiajie FANG[1*], Ahmad ALHASKAWI[2*], Yanzhao DONG[2], Cheng CHENG[1,3], Zhijie XU[1,3], Junjie TIAN[1,3], Sahar Ahmed ABDALBARY[4,5], Hui LU[2,6✉]

[1]*Department of Urology, the First Affiliated Hospital, School of Medicine, Zhejiang University, Hangzhou 310006, China*
[2]*Department of Orthopedics, the First Affiliated Hospital, School of Medicine, Zhejiang University, Hangzhou 310006, China*
[3]*Zhejiang Engineering Research Center for Urinary Bladder Carcinoma Innovation Diagnosis and Treatment, Hangzhou 310024, China*
[4]*Department of Orthopedic Physical Therapy, Faculty of Physical Therapy, Nahda University, Beni Suef 62511, Egypt*
[5]*Biomechanics and Microsurgery Labs, Nahda University, Beni Suef 62511, Egypt*
[6]*Alibaba-Zhejiang University Joint Research Center of Future Digital Healthcare, Zhejiang University, Hangzhou 310058, China*

Abstract: Prostate cancer is the second most common cancer in men, accounting for 14.1% of new cancer cases in 2020. The aggressiveness of prostate cancer is highly variable, depending on its grade and stage at the time of diagnosis. Despite recent advances in prostate cancer treatment, some patients still experience recurrence or even progression after undergoing radical treatment. Accurate initial staging and monitoring for recurrence determine patient management, which in turn affect patient prognosis and survival. Classical imaging has limitations in the diagnosis and treatment of prostate cancer, but the use of novel molecular probes has improved the detection rate, specificity, and accuracy of prostate cancer detection. Molecular probe-based imaging modalities allow the visualization and quantitative measurement of biological processes at the molecular and cellular levels in living systems. An increased understanding of tumor biology of prostate cancer and the discovery of new tumor biomarkers have allowed the exploration of additional molecular probe targets. The development of novel ligands and advances in nano-based delivery technologies have accelerated the research and development of molecular probes. Here, we summarize the use of molecular probes in positron emission tomography (PET), single-photon emission computed tomography (SPECT), magnetic resonance imaging (MRI), optical imaging, and ultrasound imaging, and provide a brief overview of important target molecules in prostate cancer.

Key words: Molecular imaging; Prostate cancer; Nuclear medicine; Prostate-specific membrane antigen (PSMA); Nanoparticle

1 Introduction

Prostate cancer is the second most commonly diagnosed cancer in men. It accounted for 14.1% of newly diagnosed cancer cases among males worldwide in 2020 but its incidence and mortality differ from country to country (Sung et al., 2021). The aggressiveness of prostate cancer varies widely. Among newly diagnosed prostate cancer cases, 80% have localized diseases, 12% regional diseases, and 4% distant metastatic diseases (Brawley, 2012). The diagnosis of diseases affects the management and prognosis of the patients. Although localized prostate cancer usually has a better prognosis, with 5-year survival rates of more than 90%, cancer recurrence is still possible even after radical therapy (Parker et al., 2020). About 15% of prostate cancer patients are diagnosed with high-risk diseases (Cooperberg et al., 2010), and many have metastases at primary diagnosis, with higher rates of treatment failure and mortality. Therefore, understanding the aggressiveness of the disease, accurate detection, and staging is crucial for prostate cancer management. Prostate cancer is often insidious and patients may not exhibit apparent malignant abnormality even in the advanced stages of the disease. The conventional techniques used to diagnose prostate cancer, such as the serum prostate-specific antigen (PSA) test and digital rectal examination (DRE), are not entirely effective

✉ Hui LU, huilu@zju.edu.cn
* The two authors contributed equally to this work
Hui LU, https://orcid.org/0000-0002-5921-1043

Received Aug. 29, 2023; Revision accepted Nov. 30, 2023;
Crosschecked Dec. 25, 2024; Published online Jan. 15, 2025

because of their low accuracy and sensitivity (Tan et al., 2023). Imaging plays an important role in the detection and treatment of prostate cancer. Although ultrasound, computed tomography (CT), and magnetic resonance imaging (MRI) still play a prominent role in prostate cancer diagnostics, clinically these approaches use morphological/functional imaging with non-specific contrast. Conventionally, newly diagnosed prostate cancer is assessed mainly through an advanced radionuclide bone scan, transrectal ultrasound (TRUS), CT, positron emission tomography (PET), or MRI that uses molecular probes (Lindenberg et al., 2016).

The emergence of multiparametric MRI (mpMRI)/ultrasound fusion biopsy has improved the accuracy and detection rate of prostate cancer (Dorfinger et al., 2022). However, an unavoidable limitation of mpMRI is that detection is nonspecific—the detected lesions may represent inflammation, hyperplasia, or tumors. Therefore, biopsies remain indispensable for characterizing and confirming the disease. To assess the efficacy of anticancer therapy, response evaluation criteria in solid tumors (RECIST) use imaging techniques such as CT and MRI to monitor changes in tumor size (Eisenhauer et al., 2009). However, RECIST 1.1 relies totally on tumor size and does not consider changes in cellular events, which limits its application in the evaluation of novel targeted therapies (Ratain and Eckhardt, 2004). Recently, there has been significant development in functional imaging modalities for evaluating tumors from different aspects of physiology (Sadeghi-Naini et al., 2012), which is helping to optimize the treatment plans for cancer patients. Novel molecular imaging techniques have been developed to visualize the spatiotemporal distribution and biochemical processes of targets in vivo in non-invasive approaches for biological, diagnostic, and therapeutic applications (Weissleder and Mahmood, 2001). The molecular probes are essential for certain imaging modalities and have also shown potential in the diagnosis and treatment of prostate cancer. The timing and intervals for the use of molecular imaging probes in the context of prostate cancer diagnosis and treatment depend on several factors, including the initial diagnosis. When prostate cancer is suspected, the initial step often involves performing mpMRI to identify potential lesions. In cases marked by elevated PSA levels or other risk factors, subsequent prostate-specific membrane antigen (PSMA)-PET or choline-PET scans may be considered to delineate the extent of the disease. After the initial diagnosis, accurate staging is imperative to determine the extent of the disease and guide treatment decisions. PSMA-PET, choline-PET, or other imaging modalities can be used to assess regional lymph node involvement, distant metastases, and the characteristics of the primary tumor. Patients undergoing active surveillance require regular intervals of imaging to monitor disease progression. Typically, mpMRI is used for this purpose, although PET scans can be incorporated as needed based on clinical developments. Once treatment is initiated, monitoring the response to therapy becomes paramount (Jadvar, 2012; Hegde et al., 2013; Miller et al., 2018; Turpin et al., 2020).

In this review, we summarize the current roles of molecular probes in the diagnosis and treatment of prostate cancer and compare the advantages and disadvantages of different imaging modalities. We also introduce potential emerging imaging techniques for prostate cancer. Representative modalities of molecular imaging include PET, CT, single-photon emission computed tomography (SPECT), MRI, optical imaging, ultrasound imaging, and multimodal imaging. Molecular probes can be antibodies, antibody segments, or peptides targeting cancer biomarkers, or small molecules that target specific enzymes, receptors, antigens, or transporters and interact with the targeted environment to reveal cancer at the molecular and cellular levels (Parker et al., 2020; Ferro et al., 2021; Yuan et al., 2022; Cheng et al., 2023). PSMA is found mainly in prostate cancer cells and provides an advanced method for assessing tumor cells and their response to treatment. The use of molecular probes contributes to obtaining cancer-specific imaging signals and achieving better imaging results.

2 Molecular probes for PET

PET uses radiotracers to visualize tumors with high sensitivity and is considered the gold standard for clinical imaging sensitivity. The basic principle of PET is that radionuclides emit positrons when decaying. The positrons travel a short distance and are annihilated with electrons to create two 511-keV photons arising at an angle of 180° (Basu et al., 2014). Rings of detectors are used to detect the emitted gamma

rays and determine the location of annihilation events through coincidence detection.

Common radionuclides available for PET imaging include fluorine-18 [^{18}F], carbon-11 [^{11}C], and radiometals such as gallium-68 [^{68}Ga], copper-64 [^{64}Cu], and zirconium-89 [^{89}Zr]. For clinical and research applications, ^{18}F is most commonly used due to its suitable half-life ($T_{1/2}$=1.8 h), positron yield, and associated detection sensitivity (Sanchez-Crespo, 2013).

2.1 ^{18}F-fluorodeoxyglucose, ^{18}F-choline, and ^{11}C-choline

^{18}F-fluorodeoxyglucose (^{18}F-FDG), ^{18}F-choline, and ^{11}C-choline are commonly used radiotracers for PET. The ability of ^{18}F-FDG PET to detect cancer relies on elevated glucose metabolism in malignant tissues, which is partly attributed to upregulated cellular membrane glucose transporters in tumors (Macheda et al., 2005). A study had shown that the expression level of glucose transporter 1 in prostate cancer cells increases with the progression of malignancy grades (Effert et al., 2004). For prostate cancer, ^{18}F-FDG PET imaging is more sensitive in less well differentiated tumors. Thus, ^{18}F-FDG PET is increasingly used to evaluate high-Gleason-score, metastatic or recurrent diseases such as late castration resistant prostate cancer (CRPC), monitoring or predicting the responses to androgen deprivation therapy (ADT) or other treatments (Mena et al., 2021). However, false negative results, owing to the non-specific uptake by normal tissue, benign prostatic hyperplasia (BPH) as well as other pathological conditions such as inflammation, compromise the specificity of ^{18}F-FDG PET, limiting its value in the diagnosis and staging of clinically organ-confined disease (Jadvar, 2011; Yu et al., 2023). Prostate cancer cells overexpress choline kinase, which is involved in the synthesis of phosphatidylcholine from choline and serves as a marker of tumor progression (Asim et al., 2016). ^{11}C- or ^{18}F-radiolabeled choline PET imaging has been widely used for advanced prostate cancer detection and shows great performance in detecting bone lesions. However, negative results from choline PET do not confirm the absence of bone metastases, and the sensitivity of choline PET is insufficient compared with novel imaging probes (Jadvar, 2011).

In summary, ^{18}F-choline PET and ^{11}C-choline PET are designed to exploit the heightened choline metabolism within prostate cancer cells. They serve as effective tools for the detection of primary tumors, assessment of lymph node metastases, and evaluation of therapeutic responses.

2.2 ^{18}F-fluciclovine

Anti-1-amino-3-^{18}F-fluorocyclobutane-1-carboxylic acid (anti-3-^{18}F-FACBC), also known as ^{18}F-fluciclovine, is a synthetic leucine analogue that interacts with amino acid transporters overexpressed in prostate cancer. It has a pharmacokinetic profile of delayed excretion, which contributes to urologic imaging assays (Asano et al., 2011; Ren et al., 2016). In a comparative study including 50 patients with recurrent prostate cancer, ^{18}F-fluciclovine performed better than choline in terms of detection rate (Nanni et al., 2015). The results of pre-salvage radiotherapy (SRT) ^{18}F-fluciclovine PET/CT imaging can help optimize treatment decisions and planning for men experiencing recurrence of prostate cancer after radical prostatectomy. These findings are also predictive of post-SRT failure-free survival. A negative ^{18}F-fluciclovine PET/CT result indicates a lower risk of failure, while the presence of pelvic nodal recurrence suggests the highest risk of SRT failure (Mena et al., 2021; Lawal et al., 2023). Many studies have assessed the effect of ^{18}F-fluciclovine PET/CT in detecting biochemical recurrence (BCR) of prostate cancer in patients who have very low levels of PSA (≤0.3 ng/mL). Results show that ^{18}F-fluciclovine PET/CT imaging is particularly better at detecting the BCR of prostate cancer, with a higher rate of positive results (96.7%) (Pernthaler et al., 2019; Marcus et al., 2021; Filippi et al., 2022). Other clinical studies have reported high specificity (75.9%) and high sensitivity (86.3%) of ^{18}F-fluciclovine PET/CT for detecting prostate cancer recurrence (Laudicella et al., 2019; Filippi et al., 2022). On the other hand, PSMA PET/CT has demonstrated higher diagnostic precision in detecting the recurrence and metastasis of prostate cancer compared to ^{18}F-fluciclovine PET/CT (Mena et al., 2021; Wang R et al., 2021). Furthermore, a meta-analysis indicated that ^{68}Ga-PSMA PET/CT has the highest specificity and sensitivity, similar to those of ^{18}F-fluciclovine PET/CT, in detecting biochemically recurrent prostate cancer at different PSA levels (Sathianathen et al., 2019). Finally, ^{18}F-PSMA analogs may be more advantageous because they offer a higher physical spatial resolution and have a longer half-life (Giesel et al., 2017).

2.3 PSMA-targeted probes

There has been a persistent effort to develop novel PET probes for use in prostate cancer diagnosis, and PSMA is one of the most focused targets.

PSMA is a 750-amino acid (aa) protein belonging to the type II transmembrane glycoprotein family. It consists of an intracellular domain (1–19 aa), a transmembrane domain (20–43 aa), and an extracellular domain (44–750 aa) (de Vincentis et al., 2019). PSMA is expressed at very low levels in normal prostatic epithelial cells as well as non-prostatic tissues including the renal cortex, duodenum, ileum, salivary gland, and lacrimal gland with activities of folate hydrolase and *N*-acetyl-α-link acidic dipeptidase (O'Keefe et al., 1998; Kinoshita et al., 2006). However, the expression of PSMA is 100–1000 times higher in prostate cancer tissues than in normal tissues (Kinoshita et al., 2006). Histopathological evaluations have found that PSMA expression is upregulated in high-grade or metastatic diseases and increases as the disease progresses (Silver et al., 1997; Bostwick et al., 1998; Ross et al., 2003). Therefore, PSMA is a significant target for imaging diagnosis of prostate cancer and its metastasis.

The effect of prior treatments on the results of molecular imaging probes in the management of prostate cancer is a complex and critical consideration. Following surgical removal of the prostate gland, PSA levels can fluctuate significantly, potentially affecting the utility of some molecular imaging probes. It is often necessary to allow several months for PSA levels to stabilize, thereby enhancing the accuracy of post-prostatectomy imaging. The administration of radiation therapy can also affect PSA levels and the efficacy of specific imaging probes. It is crucial to coordinate the timing of imaging studies with the patient's radiation treatment schedule. ADT, a cornerstone of prostate cancer treatment, can modulate the expression of certain prostate cancer biomarkers. This modulation can impact the accuracy of molecular imaging probes. The timing of imaging during ADT must be meticulously planned to ensure diagnostic precision (Hricak et al., 2007; Combes et al., 2022; Tremblay et al., 2023).

Currently, monoclonal antibodies (mAbs), peptides, and small-molecule inhibitors are important PSMA-targeted radiopharmaceutical backbones (Fig. 1). PSMA mAbs can be classified into two types: those targeting the intracellular domain and those targeting the extracellular domain of PSMA. The initial clinical attempts at PSMA-targeted imaging involved the use of a radiolabeled murine mAb, ^{111}Indium-7E11-C5.3 (^{111}In-ProstaScint®, capromab pendetide). In 1996, this mAb was approved by the US Food and Drug Administration (FDA) as a diagnostic imaging agent for prostate cancer. Unfortunately, the antibody targets the intracellular epitope of PSMA and often fails to bind to the intracellular domain due to insufficient endocytosis, thus lacking sensitivity and specificity (Sodee et al., 2000). Recent developments in PSMA-targeted imaging involve mainly small-molecule ligands, including phosphorous-based, thiol-based, and urea-based PSMA inhibitors (iPSMAs) (Table 1). Most of these bind to the active substrate recognition site of the folate hydrolase enzyme located in the extracellular domain (Maurer et al., 2016; Mena et al., 2021). Small-molecule inhibitors that can interact with PSMA have been recognized as preferred choices for molecular imaging and prostate cancer-targeted therapy (He et al., 2022). ^{68}Ga-radiolabeled small-molecule tracers include PSMA-HBED-CC (*N*,*N*'-bis[2-hydroxy-5-(carboxyethyl)benzyl]ethylenediamine-*N*,*N*'-diacetic acid), also termed ^{68}Ga-PSMA-11, ^{68}Ga-PSMA-617, ^{68}Ga-PSMA-I&T, and ^{68}Ga-P16-093 (Schmuck et al., 2017; Kuten et al., 2020; Wang et al., 2022; Schollhammer et al., 2023). Among these, ^{68}Ga-PSMA-11, binding to the extracellular domain of PSMA with high affinity based on its urea backbone, has become one of the most commonly used radiotracers in PET imaging for prostate cancer. It shows excellent

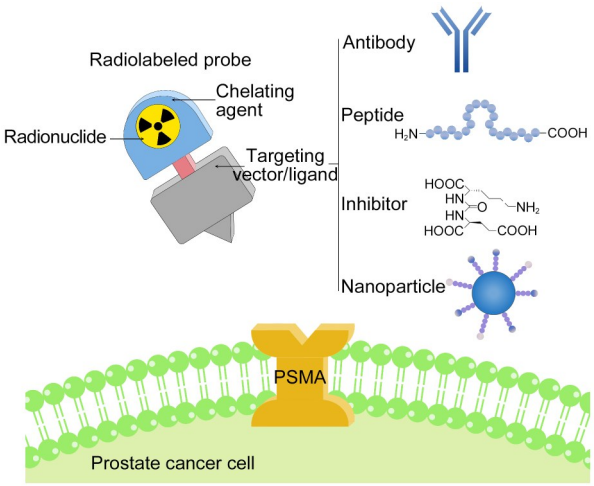

Fig. 1 Prostate-specific membrane antigen (PSMA)-targeted radiolabeled probes for prostate cancer.

Table 1 PSMA-targeted imaging radiopharmaceuticals under clinical investigation in prostate cancer

Imaging modality	Radiopharmaceutical	Radionuclide	Number of recent clinical trials*
PET	PSMA-11	^{68}Ga	71
	PSMA-11	^{18}F	3
	DCFPyL	^{18}F	31
	PSMA-1007	^{18}F	12
	rhPSMA-7.3	^{18}F	6
	PSMA-617	^{68}Ga	4
	P16-093	^{68}Ga	4
	CTT1057	^{18}F	3
	THP-PSMA	^{68}Ga	1
	PSMA-R2	^{68}Ga	1
	PSMA-BCH	^{18}F	1
	P15-041	^{68}Ga	1
	P137	^{68}Ga	1
	NY108	^{68}Ga	1
	NOTA-PSMA-PEG-Cy5.5-C	^{64}Cu	1
	SAR-bisPSMA	^{64}Cu	1
	PSMA-I&T	^{64}Cu	1
	TLX592	^{64}Cu	1
SPECT	PSMA-I&S	^{99m}Tc	2
	P137	^{99m}Tc	1
	PSMA-I&T	^{111}In	1

PET: positron emission tomography; PSMA: prostate-specific membrane antigen; SPECT: single-photon emission computed tomography; ^{68}Ga: gallium-68; ^{18}F: fluorine-18; ^{64}Cu: copper-64; ^{99m}Tc: technetium-99m; ^{111}In: indium-111. * Ongoing/recruiting trials started from January 1, 2018 to March 22, 2023, according to clinicaltrials.gov.

performance in detecting lymph nodes and distant metastases, accurately staging prostate cancer, and localizing recurrent prostate cancer even at low PSA levels, and is widely available (Prasad et al., 2016). In intermediate- or high-risk patients, the presence of nodal or distant metastases needs to be determined before radical treatment can be administered. Conventional imaging with CT and a bone scan is not sufficient to identify metastases in lymph nodes or distant organs, especially in populations with low serum PSA levels (O'Sullivan et al., 2003). According to the American Society of Clinical Oncology guidelines, PSMA PET/CT is recommended for the evaluation of high-risk locally advanced prostate cancer. A systematic review including 18 trials and 969 patients evaluated for PSMA PET in primary lymph node staging found that most trials of PSMA-targeted PET showed a weighted sensitivity of 59%, a weighted specificity of 93%, and a positive predictive value (PPV) of more than 80%, whereas trials of CT showed a weighted sensitivity of 42%, a weighted specificity of 82%, and a negative predictive value (NPV) of 32% (Petersen and Zacho, 2020). However, ^{68}Ga labeling is not always ideal, with its characteristics of short half-life, high-energy positron, and the need for on-site generators. ^{18}F labeling with, for example, 2-(3-{1-carboxy-5-[(6-[^{18}F]fluoro-pyridine 3-carbonyl)-amino]-pentyl}-ureido)-pentanedioic acid (^{18}F-DCFPyL), *N*-[*N*-[(*S*)-1,3-dicarboxypropyl]carbamoyl]-(*S*)-4-[^{18}F]fluorobenzyl-L-cysteine (^{18}F-DCFBC), or ^{18}F-PSMA-1007, is an alternative option, which can be carried out off-site because of its longer half-life (Lindenberg et al., 2020; Mena et al., 2021). ^{18}F-PSMA-1007 has lower urothelial clearance and favorable image resolution, and its performance in the initial staging of primary prostate cancer patients is comparable to that of ^{68}Ga-PSMA-11 (Fig. 2) (Chandekar et al., 2023). A meta-analysis covering 540 patients found that the overall pool detection rate was 94% per patient. The pooling median of maximal standardized uptake value (SUV_{max}) located at the intra-prostate tumor was 16, and the PPV

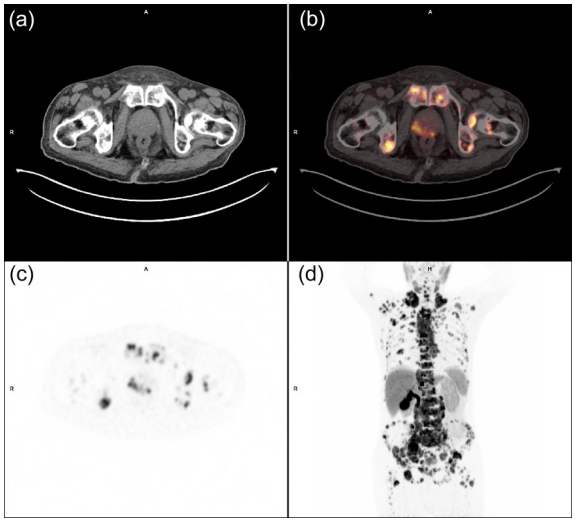

Fig. 2 ^{18}F-PSMA PET/CT findings in a 72-year-old patient. (a, b) Irregular low-density foci observed in the right peripheral area exhibited notable uptake of ^{18}F-PSMA, suggesting potential malignant changes. (c) Multiple bone mineral density foci with slightly higher ^{18}F-PSMA uptake indicated multiple bone metastatic lesions. (d) MIP showed increased ^{18}F-PSMA-1007 uptake in multiple bones and lymph nodes throughout the body, suggesting metastatic lesions. ^{18}F: fluorine-18; PSMA: prostate-specific membrane antigen; PET: positron emission tomography; CT: computed tomography; MIP: molecular insight pharmaceutical.

for each lesion was 0.90 (Huang et al., 2022). For patients who received radical prostatectomy, the presence of pelvic lymph node metastases during surgery correlated to biochemical failures (Bianco et al., 2005). A recent phase III clinical trial including 764 patients evaluated the accuracy of ^{68}Ga-PSMA-11 PET in detecting pelvic lymph node metastases and reported a diagnostic sensitivity of 0.40 and specificity of 0.95 (Hope et al., 2021). PMSA PET also plays a crucial role in the diagnosis of BCR and detection of a persistent biochemical environment after local radical treatment. ^{68}Ga-PMSA PET has been approved by the FDA for use in BCR detection after radical prostatectomy or radiotherapy. The scan positivity of ^{68}Ga-PSMA PET in BCR patients varies with serum PSA levels. For PSA categories 0–0.2, 0.2–1.0, 1.0–2.0, and >2.0 ng/mL, the positive scan rates were 42%, 58%, 76%, and 95%, respectively (Perera et al., 2016). Another study reported the performance of three ^{18}F-labeled imaging methods, namely ^{18}F-choline, ^{18}F-fluciclovine, and ^{18}F-PSMA PET/CT, in BCR detection. ^{18}F-PSMA PET/CT showed the highest detection rate, especially under the condition of low PSA levels (Wang R et al., 2021). Another systematic review comprising 1022 prostate cancer patients concluded that the diagnostic rate (DR) of ^{18}F-PSMA-1007 PET/CT for BCR ranged from 47% to 100%, with a pooled estimate of 86% (95% confidence interval (CI): 76%–95%) (Liu et al., 2022).

In addition, PSMA PET/CT may be useful in guiding surgical assessment. In a cohort including 364 patients with recurrent oligometastatic prostate cancer, 343 (94%) had metastatic lesions resected with an acceptable incidence of advanced complications (Knipper et al., 2023). Although this study did not provide evidence of prolonged survival, it provided patients with longer BCR-free survival and improved treatment-free survival. PSMA PET imaging has also shown promise for guiding salvage radiation therapy (Calais et al., 2018). In patients with PSA levels of 4 ng/mL, ^{68}Ga PSMA PET/CT-guided targeted biopsies provide a higher diagnostic yield while maintaining a better safety profile (Table 2) (Kumar et al., 2022). ^{177}Lu-PSMA-617 is an effective treatment for metastatic CRPC (mCRPC), effectively improving PSA response rates and progression-free survival in patients. ^{68}Ga-PSMA PET provides imaging parameters that can serve as prognostic biomarkers in this patient population and help to optimize ^{177}Lu-PSMA-617 treatment options (Cook et al., 2023; Pathmanandavel et al., 2023).

2.4 Androgen receptor-targeted probes

The androgen receptor (AR) plays a crucial role as a transcription factor in the regulation of prostate cancer growth. It binds to ligands such as dihydrotestosterone in the cytoplasm, activated through phosphorylation and dimerization, promoting translocation into the nucleus and regulating the expression of downstream AR-targeting genes. As the disease progresses, especially during the castration resistant phase, cancer cells may become unresponsive to ADT. Given the central role of the AR axis in mCRPC and its treatment, non-invasive probes capable of detecting the efficacy of AR axis-targeted drugs are needed. ^{18}F-fluoro-5α-dihydrotestosterone (FDHT) is a radiolabeled dihydrotestosterone analogue that allows imaging of the primary molecular driver of CRPC cancer with

Table 2 An exploration of PSMA-targeted probes used in clinical practice for prostate cancer, including an assessment of their respective advantages and limitations

Molecular probe	Purpose	Advantage	Limitation
^{18}F-FDG PET/CT	Diagnosis (rarely) and treatment	Detecting aggressive tumors	Limited sensitivity for prostate cancer
^{18}F-choline PET/CT	Diagnosis and treatment	Detecting prostate cancer lesions	Limited specificity for small lesions
^{11}C-choline PET/CT	Diagnosis and treatment	Being good for staging and restaging	Short half-life (20 min)
^{18}F-PSMA PET/CT	Diagnosis and treatment	Having high sensitivity and specificity	Limited availability and cost
^{68}Ga PSMA PET/CT	Diagnosis and treatment	Being widely used, with a high detection rate	Limited availability and cost

PSMA: prostate-specific membrane antigen; ^{18}F: fluorine-18; FDG: fluorodeoxyglucose; PET: positron emission tomography; CT: computed tomography; ^{11}C: carbon-11; ^{68}Ga: gallium-68.

PET/CT, showing high reproducibility and good interobserver reproducibility of uptake metrics (Vargas et al., 2018). It has been tested in early clinical trials of second-generation anti-androgen therapies such as enzalutamide and apalutamide (Beattie et al., 2010; Rathkopf et al., 2013). When comparing ^{18}F-FDHT and ^{18}F-FDG in mCRPC patients, those with lesions showing higher ^{18}F-FDHT uptake were found to have significantly shorter overall survival, whereas ^{18}F-FDG uptake was not associated with overall survival (Vargas et al., 2014). ^{18}F-FDHT is a promising imaging agent that contributes to our understanding of the dynamic changes occurring in metastatic prostate cancer cells. However, it does not yet provide better sensitivity than other imaging agents for the detection of recurrent or metastatic disease and needs to be further developed.

2.5 Gastrin-releasing peptide receptor-targeted probes

The gastrin-releasing peptide (GRP) receptor (GRPR) is another available molecular imaging target. Bombesin, a 14-aa natural peptide, and its human counterpart GRP regulate many physiological functions of the gastrointestinal tract and central nervous system. It influences pathophysiological processes of growth and differentiation in several human cancers, including colon, pancreatic, and prostate cancers (Mansi et al., 2013). Human GRPR binds to GRP with high affinity and has been reported to be overexpressed in 63%–100% of primary prostate cancer lesions and in 50%–85% of lymph node and bone metastases, while it is expressed at low levels in BPH and normal prostate tissue (Mansi et al., 2013; Gai et al., 2020). Thus, radiolabeled bombesin can be used to image GRPR as a receptor agonist (Wieser et al., 2014). Meanwhile, GRPR antagonists have a higher tumor-to-background ratio and higher sensitivity, and do not induce adverse effects (Baratto et al., 2018). ^{68}Ga-RM2 is the most widely reported reagent with histology as the gold standard for detecting primary prostate cancer with 89% sensitivity, 81% specificity, and 83% accuracy. The sensitivity of detecting lymph node metastases is 70% (Mena et al., 2021). Little is known about the expression of GRPR in advanced, hormone-deficient, or depression-resistant primary tumors or metastases.

2.6 Urokinase-type plasminogen activator-targeted probes

The serine protease urokinase-type plasminogen activator (uPA) and its receptor (uPAR) have been shown to play an important role in tumor metastasis and invasion. uPAR is consistently upregulated in several human cancers, including prostate cancers and bladder cancers, and is associated with advanced disease and poor prognosis (Persson et al., 2015). Radiolabeled uPAR reagents containing ^{64}Cu, ^{68}Ga, and ^{18}F have been developed and used for PET imaging in human heterozygous prostate cancer models. ^{64}Cu-DOTA-AE105 is a radiolabeled uPAR high-affinity peptide base antagonist. Initial results from its first phase I clinical trial are encouraging and support the case for larger clinical trials (Persson et al., 2015). Another probe, ^{64}Cu-NOTA-AE105, also shows good safety and stability and is able to accumulate in both primary and metastatic tumor foci (Skovgaard et al., 2017). In addition, SUV measurements from uPAR PET in primary tumors showed a significant correlation with Gleason scores, promising to reduce the need for repeated biopsies in active surveillance (Fosbøl et al., 2021).

2.7 Fibroblast activation protein-targeted probes

Fibroblast activation protein (FAP) is a type II integral membrane glycoprotein involved in extracellular matrix (ECM) remodeling and fibril formation. FAP expression is barely detectable in normal tissues but accumulates significantly in the stroma of many solid tumors (Peltier et al., 2022). In addition, overexpression of FAP in solid tumors is usually predictive of a poor prognosis (Liu et al., 2015). Recent development of FAP inhibitors (FAPIs) has made molecular imaging targeting FAP a promising modality for disease detection. Radiolabeled FAPIs such as ^{68}Ga-FAPI-04 show good performance in the diagnosis of bone metastases from malignant tumors (Dong et al., 2023). Bone disease is also a common complication of advanced prostate cancer. ^{68}Ga-FAPI-04 has a moderate uptake (SUV_{max}=6–12) in prostate cancer (Kratochwil et al., 2019) and can be used to detect primary prostate cancer and bone metastases by PET/CT (Tatar et al., 2023). Comparing ^{68}Ga-FAPI-04, ^{68}Ga-PSMA, and ^{18}F-FDG PET/CT in mCRPC patients, the combination of FAPIs with PSMA PET ensured that more heterogeneous prostate cancer lesions could be

detected (Isik et al., 2022). Preclinical studies with another probe, ^{89}Zr-B12-IgG, showed high uptake and long residency of the probe in prostate cancer tissues for 72 h by PET imaging, and demonstrated rapid blood clearance within 24 h (Hintz et al., 2020). Overall, PSMA PET has undisputed clinical value in recurrent prostate cancer, demonstrating higher sensitivity and specificity than conventional imaging in identifying distant metastatic diseases such as lymph node and bone metastases. Several imaging modalities targeting other molecules have their advantages under different conditions. The inherent advantages of PET imaging include its high sensitivity and quantifiable imaging parameters such as SUV. The combination of PET with other imaging modalities such as CT and MRI allows the integration of anatomical and functional imaging information, which can be used to assess the molecular characteristics of tumors with highly accurate anatomical structure correction (Table 3).

3 Molecular probes for SPECT

SPECT is another nuclear imaging modality that relies on radiotracers that emit individual photons during the nuclear decay process. The emitted individual photons are then detected by the gamma camera. Traditionally, gamma cameras enable planar imaging through photon-to-optical signal-to-electrical signal conversion. In modern molecular imaging applications, they rotate around the patient to create tomographic images, known as SPECT (Bai et al., 2023). Compared with PET, SPECT has no advantage in spatial resolution or sensitivity for tumor detection and is much less easily quantifiable. However, the combination of SPECT/CT has made significant progress in the field of nuclear medicine imaging. This is because it enables high-quality attenuation correction and co-registration/fusion of metabolic and anatomical images. In addition, due to the wider choice of radiopharmaceuticals and better availability of SPECT, it remains a commonly used technique in clinical practice and has significant value in the evaluation of pathology. SPECT technique is now widely used for stroke, seizure, bone disease, infection, and tumor diagnosis (Israel et al., 2019). It provides more accurate metabolic or functional information and has the ability to compare altered tracer distribution with anatomical structures, therefore enabling better diagnostic imaging (Israel et al., 2019; Crișan et al., 2022). The radioisotopes commonly used in

Table 3 General summary of the molecular probes for PET in prostate cancer

Probe/tracer	Targeted biomolecule	Imaging modality	Key advantage	Clinical application
PSMA-targeted probes	PSMA	PET/CT, PET/MRI	Remarkable sensitivity and specificity	Precise staging, restaging, detection of recurrence
AR-targeted probes	AR	PET/CT, PET/MRI	Visualization of heterogeneous AR expression	AR profiling, monitoring therapy response
GRPR-targeted probes	GRPR	PET/CT, PET/MRI	Detection of overexpressed GRPR	Imaging GRPR-positive lesions
uPAR-targeted probes	uPAR	PET/CT, PET/MRI	Non-invasive uPAR expression assessment	Tumor characterization, therapy monitoring
FAP-targeted probes	FAP	PET/CT, PET/MRI	Visualization of tumor-associated fibroblasts	Comprehensive tumor profiling, treatment response
^{18}F-FACBC	Amino acid transport	PET/CT	Enhanced lesion detection, minimal urinary excretion	Accurate staging, recurrence assessment
^{18}F-FDG	Glucose metabolism	PET/CT	Assessment of tumor glucose metabolism	Particularly in high-metabolic malignancies
^{18}F-choline	Choline metabolism	PET/CT	Detection of aberrant choline metabolism	Accurate staging, recurrence assessment
^{11}C-choline	Choline metabolism	PET/CT	Equivalent to ^{18}F-choline with shorter half-life	Accurate staging, recurrence assessment

^{18}F: fluorine-18; ^{11}C: carbon-11; PSMA: prostate-specific membrane antigen; AR: androgen receptor; GRPR: gastrin-releasing peptide receptor; uPAR: urokinase plasminogen activator receptor; FAP: fibroblast activation protein; ^{18}F-FACBC: amino-3-^{18}F-fluorocyclobutane-1-carboxylic acid; FDG: fluorodeoxyglucose; PET: positron emission tomography; CT: computed tomography; MRI: magnetic resonance imaging.

SPECT imaging are iodine-123 [^{123}I], technetium-99m [^{99m}Tc], and indium-111 [^{111}In], which emit photons of different energies (Table 4). ^{99m}Tc decays into ^{99}Tc and releases photons of appropriate energy (140.5 keV) for gamma camera imaging without imposing an additional radiation burden on the patient thanks to being a pure gamma emitting radionuclide with a short half-life ($T_{1/2}$=6 h). ^{99m}Tc-labeled radiopharmaceuticals are the imaging agents most used in nuclear medicine worldwide, with a wide range of applications in thyroid, bone, kidney, myocardial perfusion, intestine, brain, liver, and brain imaging (Papagiannopoulou, 2017). In the diagnosis of prostate cancer, ^{99m}Tc-labeled diphosphate bone scintigraphy is a widely used and high-sensitive method for detecting bone metastases. The possibility of abnormal bone scintigraphy is positively correlated with clinical stage, Gleason score, and PSA concentration. The main advantages of bone scintigraphy are its high sensitivity, low cost, and ability to measure the entire bone. Planar bone scintigraphy using ^{99m}Tc methylene diphosphonate (^{99m}Tc-MDP) is the standard imaging modality for detecting bone metastases. Unfortunately, radiotracers also accumulate in benign bone lesions, reducing the specificity of SPECT. Sodium fluoride (NaF) is another radiopharmaceutical that targets osteoblast activity. A recent phase III clinical trial compared ^{18}F-NaF PET/CT with ^{99m}Tc-MDP SPECT in high-risk prostate cancer and breast cancer patients. In a patient-based analysis, ^{18}F-NaF PET/CT showed 84.3% (95% CI: 79.9%–88.7%) accuracy vs. 77.4% (72.3%–82.5%) with ^{99m}Tc-MDP SPECT (Bénard et al., 2022). This suggests that ^{18}F-NaF has the potential to replace ^{99m}Tc-MDP as the preferred bone imaging radiopharmaceutical for patients with high-risk prostate or breast cancer. Modern technetium-labeled radiopharmaceuticals have been developed by indirect labeling using bifunctional chelators, which dope the radiometal and are linked to the pharmacophore. The pharmacophore influences the chemical properties and dictates the function of probes. This strategy has also profoundly influenced the development of ^{99m}Tc imaging agents targeting PSMA. The compound ^{99m}Tc-MIP-1404 targets PSMA via a glutamate-urea-glutamate pharmacophore and has produced promising results in early clinical trials. The compounds were cleared rapidly from the blood and localized to metastatic lesions in bone and lymph nodes within 1 h (Vallabhajosula et al., 2014). Compared to ^{68}Ga-PSMA-11 PET, the ^{99m}Tc-MIP-1404 SPECT had a similar focal SUV_{max} and higher hepatic SUV_{max} (Cook et al., 2023), though the uptakes in the liver and kidney were acceptable for imaging. ^{99m}Tc-MIP-1404 SPECT successfully detected small lesions in the prostate, bone, and lymph nodes, providing further prognostic information for both primary and biochemically recurrent tumors (Vallabhajosula et al., 2014). However, the sensitivity of ^{99m}Tc-HYNIC iPSMA in detecting PSMA lesions was 78.3%. Only lesions with SUV_{max}>20 could be successfully visualized with ^{99m}Tc-HYNIC iPSMA and only two-sevenths to one-half of lesions with SUV_{max}<20 could be detected. (Lawal et al., 2017; García-Pérez et al., 2018). This

Table 4 Overview of some molecular probes used for SPECT imaging in prostate cancer

Molecular probe	Targeted biomolecule	Key advantage	Clinical application
^{99m}Tc-MDP	Bone mineralization	Visualizes bone metastases	Staging, detecting bone metastases
^{99m}Tc-sestamibi	Mitochondrial membrane potential	Identifies active tumor regions	Assessment of tumor activity, residual disease
^{99m}Tc-MAG3	Renal function	Evaluates renal function	Assessing kidney function in patients with renal impairment
^{99m}Tc-DMSA	Renal cortical function	Detects renal cortical abnormalities	Renal imaging, assessing kidney function
^{99m}Tc-HYNIC-TOC	Somatostatin receptor expression	Images neuroendocrine tumors	Detection, staging, and restaging
^{99m}Tc-MIP-1404	PSMA expression	Visualizes PSMA-expressing tumors	Staging, restaging, detection of recurrence
^{111}In-octreotide	Somatostatin receptor expression	Detects somatostatin receptor-positive tumors	Neuroendocrine tumor imaging, detection

SPECT: single-photon emission computed tomography; ^{99m}Tc: technetium-99m; ^{111}In: indium-111; MDP: methylene diphosphonate; MAG3: mercaptoacetyltriglycine; DMSA: dimercaptosuccinic acid; HYNIC: hydrazinonicotinamide; TOC: Tyr3-octreotate; MIP: molecular insight pharmaceuticals; PSMA: prostate-specific membrane antigen.

deficiency is partly related to the low resolution of conventional SPECT cameras. Given the development of cadmium-zinc-telluride (CZT) crystal-based SPECT imaging systems, it will be possible to re-evaluate the measurement sensitivity of ^{99m}Tc-HYNIC iPSMA with new advanced, high-resolution SPECT/CT scanners. In robot-assisted surgery, the maneuverability of conventional laparoscopic gamma probes is limited. The DROP-IN gamma probe facilitates the performance of radiation-guided surgery in a robotic setting by enhancing maneuverability and surgical autonomy. A study of 25 patients compared the DROP-IN gamma probes, conventional laparoscopic gamma probes, and fluoroscopic guidance in robot-assisted sentinel lymph (SN) node dissection, expanded pelvic lymph node dissection, and prostatectomy (Dell'Oglio et al., 2021). The results showed that the DROP-IN gamma probe tracked 47 SNs in vivo, of which 100% were identified, and no adverse events were associated with its use. In vivo fluorescence imaging (FI) identified 91% of the SNs, and the laparoscopic gamma probe only 76%. In 12 patients with prostate cancer undergoing radical treatment, preoperative PET/CT revealed 64% of avid lymph nodes. The DROP-IN probe using ^{99m}Tc-PSMA-I&S detected an additional 11 metastatic lymph nodes that were not observed in preoperative PET/CT. In hospitalized patients, the DROP-IN probe had a sensitivity of 76% (95% CI: 53%–92%), specificity of 69% (95% CI: 55%–81%), PPV of 50%, and NPV of 88% (Gondoputro et al., 2022).

In addition, ^{111}In is a radioisotope with a long half-life of 2.83 d, a feature suitable for delayed imaging for diagnostic and therapeutic purposes. mAb 5D3 is a newly identified high-affinity PSMA mAb. The ^{111}In-labeled analog's pharmacokinetic properties were tested and its distribution within PSMA-positive tumors peaked at 24 h after injection and remained high until 72 h. It was significantly cleared from all organs after 192 h (Banerjee et al., 2019). This suggests that ^{111}In-5D3 can be used not only for SPECT imaging but also as an alternative to ^{177}Lu and ^{90}Y for PSMA-based radiation therapy.

4 Molecular probes for MRI

Conventional MRI is often considered an anatomical imaging modality and is primarily used to create high-resolution anatomical images of soft tissue structures such as the brain and skeletal system. MRI is based on the properties that specific atomic nuclei absorb radiofrequency energy in a strong magnetic field and align like small magnets due to their spin. In brief, MRI uses a high magnetic field and selective application of radiofrequency pulses to generate images with different signal patterns at different sites depending on the tissue components (Grover et al., 2015). MRI is an important clinical tool for identifying and characterizing prostate cancer and for evaluating the effectiveness of treatment. mpMRI-guided TRUS is an important tool for the detection of prostate cancer. Nevertheless, existing MRI tools have disadvantages in terms of sensitivity and signal-to-noise ratio compared with other methods, especially when dealing with small lesions and early-stage tumors (Zhao et al., 2019).

The development of novel contrast agents and nanoprobes is contributing to the expansion of the usability and application range of MRI. Multifunctional magnetic nanoparticles have attracted interest and have initially shown potential for molecular imaging. Iron oxide nanoparticles are characterized by long circulation and low side effects, and can be passively or actively aggregated with tumor sites through enhanced permeability and retention (EPR) effects or surface modifications. In prostate cancer diagnosis and treatment, ultrasmall superparamagnetic iron oxide (USPIO) particles have been used in clinical practice. MRI enhanced with USPIO particles, such as Combidex, a dextran-coated iron oxide nanoparticle, shows great performance in detecting suspicious lymph nodes (Fortuin et al., 2018). Iron oxide nanoparticles can be taken up by macrophages and transferred to normal lymph nodes throughout the body after intravenous dosing, but metastatic lymph nodes do not take up nanoparticles. Thus, metastatic lymph nodes can be distinguished on iron-sensitive T2*-weighted MRI sequences after administration. In a comparison between PSMA PET/CT and USPIO-MRI at 3T magnetic field strength, PSMA PET/CT identified 71 suspicious lymph nodes in 25/45 patients and USPIO-MRI identified 160 in 33/45 patients. USPIO-MRI was also more sensitive for detecting suspicious lymph nodes smaller than 5 mm (Kuten et al., 2020). Image quality is considered to be positively correlated with magnetic field strength (Heesakkers et al., 2006). The use of

ultra-high magnetic fields (7T) further improves the sensitivity of MRI and offers a better protocol for USPIO-MRI lymph node detection in prostate cancer (Fortuin et al., 2023). For diagnosis and treatment, a single imaging modality sometimes cannot cover the whole landscape of the tumor lesion. Therefore, combining nanoparticles such as USPIO with other components to construct a targeted delivery system or a multimodal imaging system is a promising solution for improvement. The upregulated transferrin (Tf) receptor (TfR) in prostate cancer is a promising target for targeted delivery systems. Zhao et al. (2019) designed a Tf-coupled USPIO nanoparticle and further enhanced tumor targeting by upregulating TfR expression. This was achieved through additional application of a gene probe encoding TfR and luciferase (Luc) driven by a prostate cancer-specific promoter differential display code 3 gene (*DD3*), which minimized off-targeting of the nanoprobe. In addition, transfection of the Luc supports FI, facilitating tumor detection through the combination of the two imaging modalities (Zhao et al., 2019).

Nerve density correlates with the aggressiveness and prognosis of prostate cancer. Superparamagnetic iron oxide neuropeptide nanoparticles coupled with propranolol can visualize nerve density in prostate cancer by MRI imaging with high sensitivity and specificity, opening up new opportunities for the study of prostate cancer (Nessler et al., 2020; You et al., 2020). Sometimes, multimodal imaging agents require complex preparation processes and have high toxicity, resulting in difficult clinical translation. Ultrafine melanin nanoparticles (MNPs) are endogenous, biodegradable materials with strong near-infrared (NIR) absorption, which can be used to construct T1-weighted MRI contrast agents through adsorption with paramagnetic metal ions (Hong et al., 2017). Xia et al. (2021) prepared a novel ultrafine MNP probe modified with PSMA-specific small-molecule inhibitors and coupled to the paramagnetic metal Mn^{2+} and ^{89}Zr for PET/MRI imaging of prostate cancer. The strong NIR absorption of the ultrafine MNPs allows the probe to be used for photoacoustic therapy and photothermal therapy (PTT). Additional labeling with iodine-131 [^{131}I] enables the probe to be used for radioisotope therapy and monitoring the treatment effect by PET/MRI, providing a platform with high loading capacity and versatile scalability (Xia et al., 2021). Besides PSMA, FAP is also a promising target for enhancing MRI. Dmochowska et al. (2023) designed and evaluated a FAP-/PSMA-targeted iron oxide nanoparticle suitable for MRI. By modifying FAP- or PSMA-targeting ligand (PSMAL) on the surface of the lymphophilic MRI reagent (FerroTrace), both FAP and PSMA nanoparticles enhanced the contrast of in situ tumors in MRI. FAP-targeted MRI also increased the proportion of pixels with elevated tumor contrast by 13% compared to PSMA (Dmochowska et al., 2023).

Generally, the ^{68}Ga-PSMA-11 PET imaging agent offers exceptional specificity for PSMA. PSMA PET is particularly valuable for the identification of small lesions, evaluation of lymph node involvement, and guiding the selection of appropriate treatment modalities. ^{18}F-DCFPyL PET is analogous to ^{68}Ga-PSMA-11 and targets PSMA, serving the same diagnostic purposes. It has gained prominence for its longer half-life, ensuring wider availability. On the other hand, mpMRI amalgamates various imaging sequences and functional data to provide a comprehensive evaluation of the prostate. It is well-suited for detecting suspicious lesions and guiding targeted biopsies.

5 Molecular probes for optical imaging

Optical imaging is considered mainly as a tool used in preclinical studies and has been applied in molecular imaging of various animal models of cancer (Kaskova et al., 2016). Benefiting from the application of nonionizing radiation, optical imaging has a safety advantage compared with other techniques using ionizing radiation such as X-rays. Optical imaging encompasses multiple sub-modalities, including bioluminescence imaging (BLI), FI, and chemiluminescence imaging (Serkova et al., 2021).

BLI generates light using Luc and substrates such as firefly Luc and luciferin (Serkova et al., 2021). Constitutive or inducible expression of Luc is used to monitor tumor growth and regression in preclinical studies of prostate cancer (Shen et al., 2020; Mease et al., 2022). Various approaches, including systemic vector delivery and adenoviral delivery biosensors, have been used for imaging prostate cancer (Adams et al., 2002). AR locus mutations and resistance to AR-axis-targeted therapies are detected using a novel adenoviral biosensor (Champagne et al., 2022). A

bioluminescent probe with the human epidermal growth factor receptor 2 (HER2)-specific affibody has been designed for detecting HER2-positive prostate cells (Bhatnagar et al., 2014; Varnosfaderani et al., 2019). FI captures emitted light from fluorescent proteins or dyes, labeling antibodies, peptides, or nanoparticles (Bai et al., 2023). Limitations of FI include autofluorescence noise from normal tissues (Serkova et al., 2021). NIR FI is highlighted for its sensitivity, safety, and low cost (Vahrmeijer et al., 2013). Fluorescence-guided surgery (FGS) using a PSMA-targeted NIR probe (OTL78) is effective for real-time tumor resection (Kularatne et al., 2019). Multimodal probes combining radionuclide and fluorescence provide high sensitivity and spatial resolution (Schottelius et al., 2019). Activatable fluorescent probes, cleaved by enzymatic activity, enhance tumor-to-normal signal ratios (Hernot et al., 2019; Eder et al., 2021). Surface-enhanced Raman scattering (SERS) is an optical imaging technique used for defining surgical boundaries (Rowe and Pomper, 2022). SERS nanoprobes targeting PSMA have been developed for high-sensitivity recognition of prostate cancer cells (Jermyn et al., 2015; Ramya et al., 2016). A beehive-inspired macroporous SERS probe captures and analyzes protein phosphorylation status in exosomes from plasma (Dong et al., 2020).

6 Molecular probes for ultrasound imaging

Ultrasound imaging is a technique that uses high-frequency sound waves to generate anatomical and functional images of organs of interest. With the advantages of high availability, non-radioactivity, and cost effectiveness, ultrasound imaging is suitable for real-time monitoring of various health conditions in clinical practice. The development and application of Doppler technology have enabled ultrasound to be widely used for assessing blood flow in tumors. However, low contrast limits the further use of ultrasound as different tissue types often have similar composition, density, and echo characteristics. To improve image quality and expand the range of applicability, several contrast agents such as microbubbles and photoacoustic imaging (PAI) probes have been developed (Table 5).

6.1 Microbubble-based probes

Microbubble contrast-enhanced ultrasound with PSMA-targeting nanobubbles shows promise in prostate cancer detection. PSMA ligands actively target PSMA-positive prostate cancer cells. Active targeting enables selective rapid accumulation in tumors and prolonged residence, visualized and quantified in real time with ultrasound (Perera et al., 2020; Wang Y et al.,

Table 5 Key characteristics and applications of microbubble-based probes and photoacoustic imaging probes

Feature	Microbubble-based probe	PAI probe
Imaging principle	Contrast-enhanced ultrasound with active targeting and acoustic cavitation	PAI using laser pulses and thermoelastic effects
Target application	Prostate cancer detection, blood flow assessment in tumors	Prostate cancer detection, imaging zinc ions in deep tissue
Targeting ligands	PSMA ligands for active targeting	Near-infrared dye and radiolabeled PSMA ligands for dual targeting
Therapeutic applications	Ultrasound-guided gene therapy with adenovirus	Multimodal activatable probes for accurate and early cancer detection
Delivery strategies	Microbubble-assisted low-frequency ultrasound for targeted delivery	Systemic administration targeting specific biomolecules
Therapeutic effects	Increased membrane permeability by acoustic cavitation effect	Combination of radioactive and activated photoacoustic signals for detection
Additional enhancements	Nanoparticles for combined therapy (PAI/FI/PTT)	Ratiometric probes for imaging zinc ions in deep tissue
Integration with other imaging techniques	Not specified	Combination with TRUS for enhanced imaging
Data analysis challenges	Not specified	Use of machine learning for analyzing physicochemical spectra

PSMA: prostate-specific membrane antigen; PAI: photoacoustic imaging; FI: fluorescence imaging; PTT: photothermal therapy; TRUS: transrectal ultrasound.

2021). In addition to being used for imaging, the acoustic cavitation effect produced by microbubbles temporarily increases membrane permeability. This enables easy passage of therapeutic agents through biological barriers like the vascular endothelium and cell membranes (Hernot and Klibanov, 2008). The use of microbubbles as carriers directly loaded with adenovirus can achieve gene therapy with a reduced clearance rate and improved translation efficiency. Meng et al. (2021) designed a nanoparticle that mimics the surface topology of viruses with IR825 working as a PAI/FI/PTT agent and sonosensitizer and Fe_3O_4 working as an MRI contrast and a photodynamic therapy (PDT)/sonodynamic therapy (SDT) enhancer. Nanoparticles combined with the microbubble-assisted low-frequency ultrasound tumor-targeted delivery strategy facilitated the aggregation of microplastics at the tumor site, and promoted PTT, PDT, and acoustic therapy. The effectiveness of the delivery strategy and the multimodal imaging capability of nanoparticles were confirmed by PAI, FI, and MRI in PC-3 tumor-bearing mouse models (Meng et al., 2021). Cyclodextrin peptide-modified and indocyanine green (ICG)-loaded vesicles can be actively delivered to tumor sites. They attach to vascular endothelial cells via cyclic arginine-glycine-aspartic (cRGD) peptide and integrin $\alpha_v\beta_3$ interaction and increase the concentration of ICG at the tumor site for more precise treatment and reduced unwanted effects (Yin et al., 2020).

6.2 PAI probes

PAI combines optical and ultrasound imaging, using laser pulses to generate ultrasound waves based on the thermoelastic effect. The absorbed energy creates ultrasound waves, detected by a transducer, reconstructing tissue absorption. A multimodal activatable probe with dual targeting for prostate cancer detection has been reported, using an NIR dye and a radiolabeled PSMAL (Li et al., 2022). PAI offers rich contrast with tunable optical wavelengths, revealing anatomical, functional, and molecular information. Limited ultrasound scattering in tissues enhances imaging depth while maintaining high resolution (Lee et al., 2015). Li et al. (2022) reported a multimodal activatable probe with dual targeting capability, consisting of an NIR dye caged by a hepsin-cleavable peptide sequence and a radiolabeled PSMAL. After systemic administration, the probe targets the tumor via PSMA-PMSAL-specific recognition and is cleaved by hepsin overexpressed by prostate cancer to generate free dye and fluoro-photoacoustic signals in situ. The accumulated radioactive and activated photoacoustic signal of probe contributes to the accurate and early detection of prostate cancer (Li et al., 2022). Zhang et al. (2021) developed ratiometric photoacoustic probes with excellent biocompatibility for in situ imaging of zinc ions in deep tissue. Targeting zinc ions, enriched in prostate cancer, these probes open new avenues for studying tumor biology involving zinc ions in vivo (An et al., 2020). TRUS is an ideal platform capable of integrating multiple molecular imaging techniques to facilitate cancer detection (Kothapalli et al., 2019; Varnosfaderani et al., 2019). The concept of endoscopic probes combining TRUS and PAI was designed and validated (Kothapalli et al., 2019), simultaneously imaging both endogenous hemoglobin and an exogenous contrast agent (ICG). Hemoglobin absorption reflected the prostate vascularity and ICG absorption was used to enhance photoacoustic contrast in the prostate. The large amount of chemical and physical information about biological tissues generated by photoacoustic spectroscopy leads to difficulties in data analysis. A promising approach is to apply machine learning to analyze the characteristic changes in photoacoustic physicochemical spectra associated with prostate cancer evolution and to establish a model for cancer diagnosis (Chen et al., 2021).

7 Other emerging molecular probes

7.1 Nanobody-based molecular probes

mAbs targeting prostate cancer markers such as PSMA have always been an option for improving the tumor specificity of probes in various imaging modalities. However, a drawback of mAbs is their poor tumor penetration. The tumor uptake of antibodies is limited by their extravasation rate, and antibodies tend to penetrate only a few layers of cells due to their relatively fast antigen-binding rates (Vasalou et al., 2015). For prostate cancer, early studies developed nanobodies targeting PSMA (Evazalipour et al., 2014; Zare et al., 2014). However, to generate nanoantibody pharmaceuticals that specifically target PSMA requires further consideration of the chemistry of the pharmacophore, the effects on antibody activity, and cell viability.

Chatalic et al. (2015) reported an ^{111}In-radiolabeled probe based on anti-PSMA nanoantibodies for SPECT/CT imaging of prostate cancer. It could be taken up and internalized by LNCap cells in vitro, and tumor lesions were clearly observed in vivo. While high renal uptake was still observed after co-injection of lysine and gelofusine, it decreased to lower levels at 3 h post-injection. In addition, the high tumor penetration characteristics of nanobodies make them suitable for the development of antibody-coupled drugs. However, the additional toxicity of antibody-drug conjugate (ADC) limits the dose administered and makes the lack of penetration of conventional antibodies more apparent (Nessler et al., 2020). The use of nanobodies as scaffolds is an alternative option to increase penetration, but with the major limitation of rapid renal clearance. Nessler et al. (2020) investigated the pharmacokinetics and efficacy of three different PSMA-targeted nanobody-potent DNA-alkylating agent conjugates. The results suggested that smaller monovalent protein scaffolds, consisting of a monovalent PSMA-binding domain and an albumin-binding domain, can improve tissue penetration and enhance in vivo efficacy in a mouse model of prostate cancer (Table 6).

7.2 Ferritin-based probes

Human ferritin is an endogenous spherical iron-binding protein consisting of 24 heavy-chain ferritin (HFn) and light-chain ferritin subunit complexes. HFn has tumor-targeting properties, mediated by TfR overexpressed in tumors. Thus, the nanocages assembled from HFn have the potential to precisely deliver small molecules, nucleic acids, proteins, or metal nanoparticles into tumors (Zhang et al., 2021). Since TfR is also upregulated on the surface of prostate cancer cells, HFn-based nanocarriers can be applied in targeted delivery of contrast agents of different imaging modalities for prostate cancer detection. The iron oxide nanoparticles encapsulated within HFn nanocages modified with fluorescein isothiocyanate (FITC) formed magnetoferritin (M-HFn) nanoparticles that bound significantly to a variety of cancer cells including prostate cancer cells (Fan et al., 2012). Another study developed ^{125}I-labeled M-HFn for SPECT/MRI imaging. This approach takes advantage of the endocytic cycling properties of TfR1 to solve the problem of nuclear imaging signal blockage caused by the high-dose injection required for MRI. High sensitivity and specificity of SPECT and MRI imaging were achieved in mice by a single injection (Tan et al., 2023).

8 Conclusions

Molecular probe-based nuclide imaging, optical imaging, and ultrasound imaging are promising

Table 6 Key features and applications of nanobody-based molecular probes and ferritin-based probes

Feature	Nanobody-based molecular probe	Ferritin-based probe
Target application	Prostate cancer detection	Prostate cancer detection
Target molecule	PSMA	TfR overexpressed in tumors
Size and structure	Small-sized monovalent protein scaffolds	Spherical nanocages assembled from 24 heavy-chain ferritin (HFn) and light-chain ferritin subunits
Tumor penetration	High penetration due to smaller size and rapid binding rates	Targeted delivery to tumors facilitated by TfR overexpression
Imaging modalities	SPECT/CT imaging	SPECT/MRI imaging
Challenges	High renal uptake, limitations in dose administration	Potential blockage of nuclear imaging signal in high-dose MRI
Enhancements	Application in antibody-coupled drugs for improved penetration	Modification with FITC, development of magnetoferritin nanoparticles
Pharmacokinetics and efficacy	Investigation of PSMA-targeted nanobody-potent DNA-alkylating agent conjugates	Encapsulation of iron oxide nanoparticles for improved SPECT/MRI
Advantages	High tissue penetration, potential improvement in in vivo efficacy	Precise delivery of contrast agents with high sensitivity and specificity
Limitations	Rapid renal clearance, potential toxicity of antibody-drug conjugates	Potential signal blockage in high-dose MRI

PSMA: prostate-specific membrane antigen; TfR: transferrin receptor; SPECT: single-photon emission computed tomography; CT: computed tomography; MRI: magnetic resonance imaging; FITC: fluorescein isothiocyanate.

approaches for the diagnosis and treatment of prostate cancer. Molecular imaging goes beyond traditional anatomical imaging modalities and provides information of biological activity at the molecular and cellular levels to deepen our understanding of tumor biology. Imaging modalities using radionuclides remain some of the most important methods in prostate cancer detection. PSMA is one of the most important molecular biomarkers of prostate cancer. The current data indicate that ^{18}F-PSMA-1007 PET/CT and ^{68}Ga-PSMA PET/CT show greater diagnostic efficacy in prostate cancer compared to ^{18}F-FDG PET/CT which is more widely used. Among these, ^{68}Ga-PSMA PET/CT exhibits a slightly higher sensitivity in diagnosing prostate cancer, while ^{18}F-PSMA-1007 PET/CT may offer higher specificity and confirmed positive rates. In addition, discoveries of AR, GRPR, and uPAR biology offer promising targets for prostate cancer imaging. SPECT has good accessibility but less sensitivity compared with PET, but new detection technologies such as CZT have renewed interest in SPECT. The use of nanomaterials in MRI, optical imaging, and ultrasound imaging has accelerated preclinical discovery. Nanotechnology allows the integration of many different materials for multimodal imaging and therapeutic functions.

Acknowledgments

This work was supported by the Medical Health Science and Technology Project of Zhejiang Provincial Health Commission (No. 2022RC146) and the Zhejiang Provincial Natural Science Foundation of China (No. LQ22H050003).

Author contributions

Jiajie FANG, Hui LU, Ahmad ALHASKAWI, and Yanzhao DONG conceptualized and investigated the manuscript. Ahmad ALHASKAWI, Sahar Ahmed ABDALBARY, and Yanzhao DONG collected data. Jiajie FANG, Ahmad ALHASKAWI, Cheng CHENG, Zhijie XU, and Junjie TIAN wrote the original draft. Sahar Ahmed ABDALBARY and Yanzhao DONG reviewed and edited the manuscript. Hui LU, Cheng CHENG, Zhijie XU, and Junjie TIAN did supervision. All authors have read and agreed to the published version of the manuscript, and therefore, have full access to all the data in the study and take responsibility for the integrity and security of the data.

Compliance with ethics guidelines

Jiajie FANG, Ahmad ALHASKAWI, Yanzhao DONG, Cheng CHENG, Zhijie XU, Junjie TIAN, Sahar Ahmed ABDALBARY, and Hui LU declare that they have no conflict of interest.

This review does not contain any studies with human or animal subjects performed by any of the authors.

References

Adams JY, Johnson M, Sato M, et al., 2002. Visualization of advanced human prostate cancer lesions in living mice by a targeted gene transfer vector and optical imaging. *Nat Med*, 8(8):891-896. https://doi.org/10.1038/nm743

An Y, Chang W, Wang W, et al., 2020. A novel tetrapeptide fluorescence sensor for early diagnosis of prostate cancer based on imaging Zn^{2+} in healthy versus cancerous cells. *J Adv Res*, 24:363-370. https://doi.org/10.1016/j.jare.2020.04.008

Asano Y, Inoue Y, Ikeda Y, et al., 2011. Phase I clinical study of NMK36: a new PET tracer with the synthetic amino acid analogue *anti*-[^{18}F]FACBC. *Ann Nucl Med*, 25(6):414-418. https://doi.org/10.1007/s12149-011-0477-z

Asim M, Massie CE, Orafidiya F, et al., 2016. Choline kinase alpha as an androgen receptor chaperone and prostate cancer therapeutic target. *J Natl Cancer Inst*, 108(5):djv371. https://doi.org/10.1093/jnci/djv371

Bai JW, Qiu SQ, Zhang GJ, 2023. Molecular and functional imaging in cancer-targeted therapy: current applications and future directions. *Signal Transduct Target Ther*, 8:89. https://doi.org/10.1038/s41392-023-01366-y

Banerjee SR, Kumar V, Lisok A, et al., 2019. Evaluation of ^{111}In-DOTA-5D3, a surrogate SPECT imaging agent for radioimmunotherapy of prostate-specific membrane antigen. *J Nucl Med*, 60(3):400-406. https://doi.org/10.2967/jnumed.118.214403

Baratto L, Jadvar H, Iagaru A, 2018. Prostate cancer theranostics targeting gastrin-releasing peptide receptors. *Mol Imaging Biol*, 20(4):501-509. https://doi.org/10.1007/s11307-017-1151-1

Basu S, Hess S, Nielsen Braad PE, et al., 2014. The basic principles of FDG-PET/CT imaging. *PET Clin*, 9(4):355-370. https://doi.org/10.1016/j.cpet.2014.07.006

Beattie BJ, Smith-Jones PM, Jhanwar YS, et al., 2010. Pharmacokinetic assessment of the uptake of 16β-^{18}F-fluoro-5α-dihydrotestosterone (FDHT) in prostate tumors as measured by PET. *J Nucl Med*, 51(2):183-192. https://doi.org/10.2967/jnumed.109.066159

Bénard F, Harsini S, Wilson D, et al., 2022. Intra-individual comparison of ^{18}F-sodium fluoride PET-CT and ^{99m}Tc bone scintigraphy with SPECT in patients with prostate cancer or breast cancer at high risk for skeletal metastases (MITNEC-A1): a multicentre, phase 3 trial. *Lancet Oncol*, 23(12):1499-1507. https://doi.org/10.1016/S1470-2045(22)00642-8

Bhatnagar A, Wang YC, Mease RC, et al., 2014. AEG-1 promoter−mediated imaging of prostate cancer. *Cancer Res*, 74(20):5772-5781. https://doi.org/10.1158/0008-5472.Can-14-0018

Bianco FJ, Scardino PT, Eastham JA, 2005. Radical prostatectomy: long-term cancer control and recovery of sexual

and urinary function ("trifecta"). *Urology*, 66(5 Suppl): 83-94.
https://doi.org/10.1016/j.urology.2005.06.116

Bostwick DG, Pacelli A, Blute M, et al., 1998. Prostate specific membrane antigen expression in prostatic intraepithelial neoplasia and adenocarcinoma: a study of 184 cases. *Cancer*, 82(11):2256-2261.
https://doi. org/10.1002/(sici)1097-0142(19980601)82:11<2256::aid-cncr22>3.0.co;2-s

Brawley OW, 2012. Trends in prostate cancer in the United States. *J Natl Cancer Inst Monogr*, 2012(45):152-156.
https://doi.org/10.1093/jncimonographs/lgs035

Calais J, Cao MS, Nickols NG, 2018. The utility of PET/CT in the planning of external radiation therapy for prostate cancer. *J Nucl Med*, 59(4):557-567.
https://doi.org/10.2967/jnumed.117.196444

Champagne A, Jain P, Vélot L, et al., 2022. A transcriptional biosensor to monitor single cancer cell therapeutic responses by bioluminescence microscopy. *Theranostics*, 12(2): 474-492.
https://doi.org/10.7150/thno.63744

Chandekar KR, Singh H, Kumar R, et al., 2023. Comparison of ^{18}F-PSMA-1007 PET/CT with ^{68}Ga-PSMA-11 PET/CT for initial staging in intermediate- and high-risk prostate cancer. *Clin Nucl Med*, 48(1):e1-e8.
https://doi.org/10.1097/rlu.0000000000004430

Chatalic KL, Veldhoven-Zweistra J, Bolkestein M, et al., 2015. A novel ^{111}In-labeled anti-prostate-specific membrane antigen nanobody for targeted SPECT/CT imaging of prostate cancer. *J Nucl Med*, 56(7):1094-1099.
https://doi.org/10.2967/jnumed.115.156729

Chen YN, Xu CD, Zhang ZY, et al., 2021. Prostate cancer identification via photoacoustic spectroscopy and machine learning. *Photoacoustics*, 23:100280.
https://doi.org/10.1016/j.pacs.2021.100280

Cheng LY, Yang TS, Zhang J, et al., 2023. The application of radiolabeled targeted molecular probes for the diagnosis and treatment of prostate cancer. *Korean J Radiol*, 24(6): 574-589.
https://doi.org/10.3348/kjr.2022.1002

Combes AD, Palma CA, Calopedos R, et al., 2022. PSMA PET-CT in the diagnosis and staging of prostate cancer. *Diagnostics (Basel)*, 12(11):2594.
https://doi.org/10.3390/diagnostics12112594

Cook GJR, Wong WL, Sanghera B, et al., 2023. Eligibility for ^{177}Lu-PSMA therapy depends on the choice of companion diagnostic tracer: a comparison of ^{68}Ga-PSMA-11 and ^{99m}Tc-MIP-1404 in metastatic castration-resistant prostate cancer. *J Nucl Med*, 64(2):227-231.
https://doi.org/10.2967/jnumed.122.264296

Cooperberg MR, Broering JM, Carroll PR, 2010. Time trends and local variation in primary treatment of localized prostate cancer. *J Clin Oncol*, 28(7):1117-1123.
https://doi.org/10.1200/jco.2009.26.0133

Crișan G, Moldovean-Cioroianu NS, Timaru DG, et al., 2022. Radiopharmaceuticals for PET and SPECT imaging: a literature review over the last decade. *Int J Mol Sci*, 23(9):5023.
https://doi.org/10.3390/ijms23095023

Dell'Oglio P, Meershoek P, Maurer T, et al., 2021. A DROP-IN gamma probe for robot-assisted radioguided surgery of lymph nodes during radical prostatectomy. *Eur Urol*, 79(1): 124-132.
https://doi.org/10.1016/j.eururo.2020.10.031

de Vincentis G, Gerritsen W, Gschwend JE, et al., 2019. Advances in targeted alpha therapy for prostate cancer. *Ann Oncol*, 30(11):1728-1739.
https://doi.org/10.1093/annonc/mdz270

Dmochowska N, Milanova V, Mukkamala R, et al., 2023. Nanoparticles targeted to fibroblast activation protein outperform PSMA for MRI delineation of primary prostate tumors. *Small*, 19(21):2204956.
https://doi.org/10.1002/smll.202204956

Dong SL, Wang YH, Liu ZQ, et al., 2020. Beehive-inspired macroporous SERS probe for cancer detection through capturing and analyzing exosomes in plasma. *ACS Appl Mater Interfaces*, 12(4):5136-5146.
https://doi.org/10.1021/acsami.9b21333

Dong YZ, Zhou HY, Alhaskawi A, et al., 2023. The superiority of fibroblast activation protein inhibitor (FAPI) PET/CT versus FDG PET/CT in the diagnosis of various malignancies. *Cancers (Basel)*, 15(4):1193.
https://doi.org/10.3390/cancers15041193

Dorfinger J, Ponholzer A, Stolzlechner M, et al., 2022. MRI/ultrasound fusion biopsy of the prostate compared to systematic prostate biopsy—effectiveness and accuracy of a combined approach in daily clinical practice. *Eur J Radiol*, 154:110432.
https://doi.org/10.1016/j.ejrad.2022.110432

Eder AC, Omrane MA, Stadlbauer S, et al., 2021. The PSMA-11-derived hybrid molecule PSMA-914 specifically identifies prostate cancer by preoperative PET/CT and intraoperative fluorescence imaging. *Eur J Nucl Med Mol Imaging*, 48(6):2057-2058.
https://doi.org/10.1007/s00259-020-05184-0

Effert P, Beniers AJ, Tamimi Y, et al., 2004. Expression of glucose transporter 1 (Glut-1) in cell lines and clinical specimens from human prostate adenocarcinoma. *Anticancer Res*, 24(5A):3057-3063.

Eisenhauer EA, Therasse P, Bogaerts J, et al., 2009. New response evaluation criteria in solid tumours: revised RECIST guideline (version 1.1). *Eur J Cancer*, 45(2):228-247.
https://doi.org/10.1016/j.ejca.2008.10.026

Evazalipour M, D'Huyvetter M, Tehrani BS, et al., 2014. Generation and characterization of nanobodies targeting PSMA for molecular imaging of prostate cancer. *Contrast Media Mol Imaging*, 9(3):211-220.
https://doi.org/10.1002/cmmi.1558

Fan KL, Cao CQ, Pan YX, et al., 2012. Magnetoferritin nanoparticles for targeting and visualizing tumour tissues. *Nat Nanotechnol*, 7(7):459-464.
https://doi.org/10.1038/nnano.2012.90

Ferro M, de Cobelli O, Vartolomei MD, et al., 2021. Prostate

cancer radiogenomics-from imaging to molecular characterization. *Int J Mol Sci*, 22(18):9971. https://doi.org/10.3390/ijms22189971

Filippi L, Bagni O, Crisafulli C, et al., 2022. Detection rate and clinical impact of PET/CT with ^{18}F-FACBC in patients with biochemical recurrence of prostate cancer: a retrospective bicentric study. *Biomedicines*, 10(1):177. https://doi.org/10.3390/biomedicines10010177

Fortuin A, van Asten J, Veltien A, et al., 2023. Small suspicious lymph nodes detected on ultrahigh-field magnetic resonance imaging (MRI) in patients with prostate cancer with high risk of nodal metastases: the first in-patient study on ultrasmall superparamagnetic iron oxide-enhanced 7T MRI. *Eur Urol*, 83(4):375-377. https://doi.org/10.1016/j.eururo.2023.01.002

Fortuin AS, Brüggemann R, van der Linden J, et al., 2018. Ultrasmall superparamagnetic iron oxides for metastatic lymph node detection: back on the block. *WIREs Nanomed Nanobiotechnol*, 10(1):e1471. https://doi.org/10.1002/wnan.1471

Fosbøl MØ, Kurbegovic S, Johannesen HH, et al., 2021. Urokinase-type plasminogen activator receptor (uPAR) PET/MRI of prostate cancer for noninvasive evaluation of aggressiveness: comparison with gleason score in a prospective phase 2 clinical trial. *J Nucl Med*, 62(3):354-359. https://doi.org/10.2967/jnumed.120.248120

Gai YK, Yuan LJ, Sun LY, et al., 2020. Comparison of Al^{18}F- and ^{68}Ga-labeled NOTA-PEG$_4$-LLP2A for PET imaging of very late antigen-4 in melanoma. *J Biol Inorg Chem*, 25(1):99-108. https://doi.org/10.1007/s00775-019-01742-6

García-Pérez FO, Davanzo J, López-Buenrostro S, et al., 2018. Head to head comparison performance of ^{99m}Tc-EDDA/HYNIC-iPSMA SPECT/CT and ^{68}Ga-PSMA-11 PET/CT a prospective study in biochemical recurrence prostate cancer patients. *Am J Nucl Med Mol Imaging*, 8(5):332-340.

Giesel FL, Hadaschik B, Cardinale J, et al., 2017. F-18 labelled PSMA-1007: biodistribution, radiation dosimetry and histopathological validation of tumor lesions in prostate cancer patients. *Eur J Nucl Med Mol Imaging*, 44(4):678-688. https://doi.org/10.1007/s00259-016-3573-4

Gondoputro W, Scheltema MJ, Blazevski A, et al., 2022. Robot-assisted prostate-specific membrane antigen-radioguided surgery in primary diagnosed prostate cancer. *J Nucl Med*, 63(11):1659-1664. https://doi.org/10.2967/jnumed.121.263743

Grover VPB, Tognarelli JM, Crossey MME, et al., 2015. Magnetic resonance imaging: principles and techniques: lessons for clinicians. *J Clin Exp Hepatol*, 5(3):246-255. https://doi.org/10.1016/j.jceh.2015.08.001

He YD, Xu WD, Xiao YT, et al., 2022. Targeting signaling pathways in prostate cancer: mechanisms and clinical trials. *Signal Transduct Target Ther*, 7:198. https://doi.org/10.1038/s41392-022-01042-7

Heesakkers RAM, Fütterer JJ, Hövels AM, et al., 2006. Prostate cancer evaluated with ferumoxtran-10–enhanced T2*-weighted MR imaging at 1.5 and 3.0 T: early experience. *Radiology*, 239(2):481-487. https://doi.org/10.1148/radiol.2392050411

Hegde JV, Mulkern RV, Panych LP, et al., 2013. Multiparametric MRI of prostate cancer: an update on state-of-the-art techniques and their performance in detecting and localizing prostate cancer. *J Magn Reson Imaging*, 37(5):1035-1054. https://doi.org/10.1002/jmri.23860

Hernot S, Klibanov AL, 2008. Microbubbles in ultrasound-triggered drug and gene delivery. *Adv Drug Deliv Rev*, 60(10):1153-1166. https://doi.org/10.1016/j.addr.2008.03.005

Hernot S, van Manen L, Debie P, et al., 2019. Latest developments in molecular tracers for fluorescence image-guided cancer surgery. *Lancet Oncol*, 20(7):e354-e367. https://doi.org/10.1016/S1470-2045(19)30317-1

Hintz HM, Gallant JP, Vander Griend DJ, et al., 2020. Imaging fibroblast activation protein alpha improves diagnosis of metastatic prostate cancer with positron emission tomography. *Clin Cancer Res*, 26(18):4882-4891. https://doi.org/10.1158/1078-0432.Ccr-20-1358

Hong SH, Sun Y, Tang C, et al., 2017. Chelator-free and biocompatible melanin nanoplatform with facile-loading gadolinium and copper-64 for bioimaging. *Bioconjugate Chem*, 28(7):1925-1930. https://doi.org/10.1021/acs.bioconjchem.7b00245

Hope TA, Eiber M, Armstrong WR, et al., 2021. Diagnostic accuracy of ^{68}Ga-PSMA-11 PET for pelvic nodal metastasis detection prior to radical prostatectomy and pelvic lymph node dissection: a multicenter prospective phase 3 imaging trial. *JAMA Oncol*, 7(11):1635-1642. https://doi.org/10.1001/jamaoncol.2021.3771

Hricak H, Choyke PL, Eberhardt SC, et al., 2007. Imaging prostate cancer: a multidisciplinary perspective. *Radiology*, 243(1):28-53. https://doi.org/10.1148/radiol.2431030580

Huang YT, Tseng NC, Chen YK, et al., 2022. The detection performance of ^{18}F-prostate-specific membrane antigen-1007 PET/CT in primary prostate cancer: a systemic review and meta-analysis. *Clin Nucl Med*, 47(9):755-762. https://doi.org/10.1097/rlu.0000000000004228

Isik EG, Has-Simsek D, Sanli O, et al., 2022. Fibroblast activation protein–targeted PET imaging of metastatic castration-resistant prostate cancer compared with ^{68}Ga-PSMA and ^{18}F-FDG PET/CT. *Clin Nucl Med*, 47(1):e54-e55. https://doi.org/10.1097/rlu.0000000000003837

Israel O, Pellet O, Biassoni L, et al., 2019. Two decades of SPECT/CT – the coming of age of a technology: an updated review of literature evidence. *Eur J Nucl Med Mol Imaging*, 46(10):1990-2012. https://doi.org/10.1007/s00259-019-04404-6

Jadvar H, 2011. Prostate cancer: PET with ^{18}F-FDG, ^{18}F- or ^{11}C-acetate, and ^{18}F- or ^{11}C-choline. *J Nucl Med*, 52(1):81-89. https://doi.org/10.2967/jnumed.110.077941

Jadvar H, 2012. Molecular imaging of prostate cancer: PET radiotracers. *Am J Roentgenol*, 199(2):278-291. https://doi.org/10.2214/ajr.12.8816

Jermyn M, Mok K, Mercier J, et al., 2015. Intraoperative brain cancer detection with Raman spectroscopy in humans. *Sci Transl Med*, 7(274):274ra19. https://doi.org/10.1126/scitranslmed.aaa2384

Kaskova ZM, Tsarkova AS, Yampolsky IV, 2016. 1001 lights: luciferins, luciferases, their mechanisms of action and applications in chemical analysis, biology and medicine. *Chem Soc Rev*, 45(21):6048-6077. https://doi.org/10.1039/c6cs00296j

Kinoshita Y, Kuratsukuri K, Landas S, et al., 2006. Expression of prostate-specific membrane antigen in normal and malignant human tissues. *World J Surg*, 30(4):628-636. https://doi.org/10.1007/s00268-005-0544-5

Knipper S, Mehdi Irai M, Simon R, et al., 2023. Cohort study of oligorecurrent prostate cancer patients: oncological outcomes of patients treated with salvage lymph node dissection via prostate-specific membrane antigen-radioguided surgery. *Eur Urol*, 83(1):62-69. https://doi.org/10.1016/j.eururo.2022.05.031

Kothapalli SR, Sonn GA, Choe JW, et al., 2019. Simultaneous transrectal ultrasound and photoacoustic human prostate imaging. *Sci Transl Med*, 11(507):eaav2169. https://doi.org/10.1126/scitranslmed.aav2169

Kratochwil C, Flechsig P, Lindner T, et al., 2019. ^{68}Ga-FAPI PET/CT: tracer uptake in 28 different kinds of cancer. *J Nucl Med*, 60(6):801-805. https://doi.org/10.2967/jnumed.119.227967

Kularatne SA, Thomas M, Myers CH, et al., 2019. Evaluation of novel prostate-specific membrane antigen-targeted near-infrared imaging agent for fluorescence-guided surgery of prostate cancer. *Clin Cancer Res*, 25(1):177-187. https://doi.org/10.1158/1078-0432.CCR-18-0803

Kumar R, Singh SK, Mittal BR, et al., 2022. Safety and diagnostic yield of ^{68}Ga prostate-specific membrane antigen PET/CT-guided robotic-assisted transgluteal prostatic biopsy. *Radiology*, 303(2):392-398. https://doi.org/10.1148/radiol.204066

Kuten J, Fahoum I, Savin Z, et al., 2020. Head-to-head comparison of ^{68}Ga-PSMA-11 with ^{18}F-PSMA-1007 PET/CT in staging prostate cancer using histopathology and immunohistochemical analysis as a reference standard. *J Nucl Med*, 61(4):527-532. https://doi.org/10.2967/jnumed.119.234187

Laudicella R, Albano D, Alongi P, et al., 2019. ^{18}F-FACBC in prostate cancer: a systematic review and meta-analysis. *Cancers (Basel)*, 11(9):1348. https://doi.org/10.3390/cancers11091348

Lawal IO, Ankrah AO, Mokgoro NP, et al., 2017. Diagnostic sensitivity of Tc-99m HYNIC PSMA SPECT/CT in prostate carcinoma: a comparative analysis with Ga-68 PSMA PET/CT. *Prostate*, 77(11):1205-1212. https://doi.org/10.1002/pros.23379

Lawal IO, Marcus C, Schuster DM, et al., 2023. Impact of ^{18}F-fluciclovine PET/CT findings on failure-free survival in biochemical recurrence of prostate cancer following salvage radiation therapy. *Clin Nucl Med*, 48(4):e153-e159. https://doi.org/10.1097/rlu.0000000000004590

Lee C, Jeon M, Kim C, 2015. Photoacoustic imaging in nanomedicine. *In*: Hamblin MR, Avci P (Eds.), Applications of Nanoscience in Photomedicine. Woodhead Publishing, Cambridge, p.31-47. https://doi.org/10.1533/9781908818782.31

Li SH, Li Q, Chen W, et al., 2022. A renal-clearable activatable molecular probe for fluoro-photacoustic and radioactive imaging of cancer biomarkers. *Small*, 18(28):2201334. https://doi.org/10.1002/smll.202201334

Lindenberg L, Ahlman M, Turkbey B, et al., 2016. Evaluation of prostate cancer with PET/MRI. *J Nucl Med*, 57(Suppl 3): 111S-116S. https://doi.org/10.2967/jnumed.115.169763

Lindenberg L, Mena E, Turkbey B, et al., 2020. Evaluating biochemically recurrent prostate cancer: histologic validation of ^{18}F-DCFPyL PET/CT with comparison to multiparametric MRI. *Radiology*, 296(3):564-572. https://doi.org/10.1148/radiol.2020192018

Liu F, Qi L, Liu B, et al., 2015. Fibroblast activation protein overexpression and clinical implications in solid tumors: a meta-analysis. *PLoS ONE*, 10(3):e0116683. https://doi.org/10.1371/journal.pone.0116683

Liu X, Jiang T, Gao CL, et al., 2022. Detection rate of fluorine-18 prostate-specific membrane antigen-1007 PET/CT for prostate cancer in primary staging and biochemical recurrence with different serum PSA levels: a systematic review and meta-analysis. *Front Oncol*, 12:911146. https://doi.org/10.3389/fonc.2022.911146

Macheda ML, Rogers S, Best JD, 2005. Molecular and cellular regulation of glucose transporter (GLUT) proteins in cancer. *J Cell Physiol*, 202(3):654-662. https://doi.org/10.1002/jcp.20166

Mansi R, Fleischmann A, Mäcke HR, et al., 2013. Targeting GRPR in urological cancers—from basic research to clinical application. *Nat Rev Urol*, 10(4):235-244. https://doi.org/10.1038/nrurol.2013.42

Marcus C, Abiodun-Ojo OA, Jani AB, et al., 2021. Clinical utility of ^{18}F-fluciclovine PET/CT in recurrent prostate cancer with very low (≤0.3 ng/mL) prostate-specific antigen levels. *Am J Nucl Med Mol Imaging*, 11(5):406-414.

Maurer T, Eiber M, Schwaiger M, et al., 2016. Current use of PSMA-PET in prostate cancer management. *Nat Rev Urol*, 13(4):226-235. https://doi.org/10.1038/nrurol.2016.26

Mease RC, Kang CM, Kumar V, et al., 2022. An improved ^{211}At-labeled agent for PSMA-targeted α-therapy. *J Nucl Med*, 63(2):259-267. https://doi.org/10.2967/jnumed.121.262098

Mena E, Black PC, Rais-Bahrami S, et al., 2021. Novel PET imaging methods for prostate cancer. *World J Urol*, 39(3): 687-699. https://doi.org/10.1007/s00345-020-03344-3

Meng ZY, Zhang Y, Shen E, et al., 2021. Marriage of virus-mimic surface topology and microbubble-assisted ultrasound for enhanced intratumor accumulation and improved cancer theranostics. *Adv Sci (Weinh)*, 8(13):2004670. https://doi.org/10.1002/advs.202004670

Miller ET, Salmasi A, Reiter RE, 2018. Anatomic and molecular imaging in prostate cancer. *Cold Spring Harb Perspect Med*, 8(3):a030619. https://doi.org/10.1101/cshperspect.a030619

Nanni C, Schiavina R, Brunocilla E, et al., 2015. ^{18}F-fluciclovine PET/CT for the detection of prostate cancer relapse: a comparison to ^{11}C-choline PET/CT. *Clin Nucl Med*, 40(8): e386-e391. https://doi.org/10.1097/rlu.0000000000000849

Nessler I, Khera E, Vance S, et al., 2020. Increased tumor penetration of single-domain antibody-drug conjugates improves *in vivo* efficacy in prostate cancer models. *Cancer Res*, 80(6): 1268-1278. https://doi.org/10.1158/0008-5472.Can-19-2295

O'Keefe DS, Su SL, Bacich DJ, et al., 1998. Mapping, genomic organization and promoter analysis of the human prostate-specific membrane antigen gene. *Biochim Biophys Acta*, 1443(1-2):113-127. https://doi.org/10.1016/s0167-4781(98)00200-0

O'Sullivan JM, Norman AR, Cook GJ, et al., 2003. Broadening the criteria for avoiding staging bone scans in prostate cancer: a retrospective study of patients at the Royal Marsden Hospital. *BJU Int*, 92(7):685-689. https://doi.org/10.1046/j.1464-410x.2003.04480.x

Papagiannopoulou D, 2017. Technetium-99m radiochemistry for pharmaceutical applications. *J Labelled Comp Radiopharm*, 60(11):502-520. https://doi.org/10.1002/jlcr.3531

Parker C, Castro E, Fizazi K, et al., 2020. Prostate cancer: ESMO Clinical Practice Guidelines for diagnosis, treatment and follow-up. *Ann Oncol*, 31(9):1119-1134. https://doi.org/10.1016/j.annonc.2020.06.011

Pathmanandavel S, Crumbaker M, Nguyen A, et al., 2023. The prognostic value of posttreatment ^{68}Ga-PSMA-11 PET/CT and ^{18}F-FDG PET/CT in metastatic castration-resistant prostate cancer treated with ^{177}Lu-PSMA-617 and NOX66 in a phase I/II trial (LuPIN). *J Nucl Med*, 64(1):69-74. https://doi.org/10.2967/jnumed.122.264104

Peltier A, Seban RD, Buvat I, et al., 2022. Fibroblast heterogeneity in solid tumors: from single cell analysis to whole-body imaging. *Semin Cancer Biol*, 86:262-272. https://doi.org/10.1016/j.semcancer.2022.04.008

Perera M, Papa N, Christidis D, et al., 2016. Sensitivity, specificity, and predictors of positive ^{68}Ga-prostate-specific membrane antigen positron emission tomography in advanced prostate cancer: a systematic review and meta-analysis. *Eur Urol*, 70(6):926-937. https://doi.org/10.1016/j.eururo.2016.06.021

Perera RH, de Leon A, Wang XN, et al., 2020. Real time ultrasound molecular imaging of prostate cancer with PSMA-targeted nanobubbles. *Nanomed Nanotechnol Biol Med*, 28:102213. https://doi.org/10.1016/j.nano.2020.102213

Pernthaler B, Kulnik R, Gstettner C, et al., 2019. A prospective head-to-head comparison of ^{18}F-fluciclovine with ^{68}Ga-PSMA-11 in biochemical recurrence of prostate cancer in PET/CT. *Clin Nucl Med*, 44(10):e566-e573. https://doi.org/10.1097/rlu.0000000000002703

Persson M, Skovgaard D, Brandt-Larsen M, et al., 2015. First-in-human uPAR PET: imaging of cancer aggressiveness. *Theranostics*, 5(12):1303-1316. https://doi.org/10.7150/thno.12956

Petersen LJ, Zacho HD, 2020. PSMA PET for primary lymph node staging of intermediate and high-risk prostate cancer: an expedited systematic review. *Cancer Imaging*, 20:10. https://doi.org/10.1186/s40644-020-0290-9

Prasad V, Steffen IG, Diederichs G, et al., 2016. Biodistribution of [^{68}Ga]PSMA-HBED-CC in patients with prostate cancer: characterization of uptake in normal organs and tumour lesions. *Mol Imaging Biol*, 18(3):428-436. https://doi.org/10.1007/s11307-016-0945-x

Ramya AN, Joseph MM, Nair JB, et al., 2016. New insight of tetraphenylethylene-based Raman signatures for targeted SERS nanoprobe construction toward prostate cancer cell detection. *ACS Appl Mater Interfaces*, 8(16):10220-10225. https://doi.org/10.1021/acsami.6b01908

Ratain MJ, Eckhardt SG, 2004. Phase II studies of modern drugs directed against new targets: if you are fazed, too, then resist RECIST. *J Clin Oncol*, 22(22):4442-4445. https://doi.org/10.1200/jco.2004.07.960

Rathkopf DE, Morris MJ, Fox JJ, et al., 2013. Phase I study of ARN-509, a novel antiandrogen, in the treatment of castration-resistant prostate cancer. *J Clin Oncol*, 31(28): 3525-3530. https://doi.org/10.1200/jco.2013.50.1684

Ren JY, Yuan LL, Wen GH, et al., 2016. The value of anti-1-amino-3-^{18}F-fluorocyclobutane-1-carboxylic acid PET/CT in the diagnosis of recurrent prostate carcinoma: a meta-analysis. *Acta Radiol*, 57(4):487-493. https://doi.org/10.1177/0284185115581541

Ross JS, Sheehan CE, Fisher HAG, et al., 2003. Correlation of primary tumor prostate-specific membrane antigen expression with disease recurrence in prostate cancer. *Clin Cancer Res*, 9(17):6357-6362.

Rowe SP, Pomper MG, 2022. Molecular imaging in oncology: current impact and future directions. *CA Cancer J Clin*, 72(4):333-352. https://doi.org/10.3322/caac.21713

Sadeghi-Naini A, Falou O, Hudson JM, et al., 2012. Imaging innovations for cancer therapy response monitoring. *Imaging Med*, 4(3):311-327. https://doi.org/10.2217/iim.12.23

Sanchez-Crespo A, 2013. Comparison of Gallium-68 and Fluorine-18 imaging characteristics in positron emission tomography. *Appl Radiat Isot*, 76:55-62. https://doi.org/10.1016/j.apradiso.2012.06.034

Sathianathen NJ, Butaney M, Konety BR, 2019. The utility of

PET-based imaging for prostate cancer biochemical recurrence: a systematic review and meta-analysis. *World J Urol*, 37(7):1239-1249. https://doi.org/10.1007/s00345-018-2403-7

Schmuck S, Mamach M, Wilke F, et al., 2017. Multiple time-point ^{68}Ga-PSMA I&T PET/CT for characterization of primary prostate cancer: value of early dynamic and delayed imaging. *Clin Nucl Med*, 42(6):e286-e293. https://doi.org/10.1097/rlu.0000000000001589

Schollhammer R, Robert G, Asselineau J, et al., 2023. Comparison of ^{68}Ga-PSMA-617 PET/CT and ^{68}Ga-RM2 PET/CT in patients with localized prostate cancer who are candidates for radical prostatectomy: a prospective, single-arm, single-center, phase II study. *J Nucl Med*, 64(3):379-385. https://doi.org/10.2967/jnumed.122.263889

Schottelius M, Wurzer A, Wissmiller K, et al., 2019. Synthesis and preclinical characterization of the PSMA-targeted hybrid tracer PSMA-I&F for nuclear and fluorescence imaging of prostate cancer. *J Nucl Med*, 60(1):71-78. https://doi.org/10.2967/jnumed.118.212720

Serkova NJ, Glunde K, Haney CR, et al., 2021. Preclinical applications of multi-platform imaging in animal models of cancer. *Cancer Res*, 81(5):1189-1200. https://doi.org/10.1158/0008-5472.Can-20-0373

Shen CJ, Minn I, Hobbs RF, et al., 2020. Auger radiopharmaceutical therapy targeting prostate-specific membrane antigen in a micrometastatic model of prostate cancer. *Theranostics*, 10(7):2888-2896. https://doi.org/10.7150/thno.38882

Silver DA, Pellicer I, Fair WR, et al., 1997. Prostate-specific membrane antigen expression in normal and malignant human tissues. *Clin Cancer Res*, 3(1):81-85.

Skovgaard D, Persson M, Brandt-Larsen M, et al., 2017. Safety, dosimetry, and tumor detection ability of ^{68}Ga-NOTA-AE105: first-in-human study of a novel radioligand for uPAR PET imaging. *J Nucl Med*, 58(3):379-386. https://doi.org/10.2967/jnumed.116.178970

Sodee DB, Malguria N, Faulhaber P, et al., 2000. Multicenter ProstaScint imaging findings in 2154 patients with prostate cancer. *Urology*, 56(6):988-993. https://doi.org/10.1016/s0090-4295(00)00824-4

Sung H, Ferlay J, Siegel RL, et al., 2021. Global cancer statistics 2020: GLOBOCAN estimates of incidence and mortality worldwide for 36 cancers in 185 countries. *CA Cancer J Clin*, 71(3):209-249. https://doi.org/10.3322/caac.21660

Tan Y, Fang ZH, Tang YX, et al., 2023. Clinical advancement of precision theranostics in prostate cancer. *Front Oncol*, 13:1072510. https://doi.org/10.3389/fonc.2023.1072510

Tatar G, Baykal Koca S, Sevindir İ, et al., 2023. ^{68}Ga-FAPI-04 PET/CT in primary signet ring-like cell carcinoma of prostate with bone metastases. *Clin Nucl Med*, 48(4):e188-e189. https://doi.org/10.1097/rlu.0000000000004550

Tremblay S, Alhogbani M, Weickhardt A, et al., 2023. Influence of molecular imaging on patient selection for treatment intensification prior to salvage radiation therapy for prostate cancer: a post hoc analysis of the PROPS trial. *Cancer Imaging*, 23:57. https://doi.org/10.1186/s40644-023-00570-x

Turpin A, Girard E, Baillet C, et al., 2020. Imaging for metastasis in prostate cancer: a review of the literature. *Front Oncol*, 10:55. https://doi.org/10.3389/fonc.2020.00055

Vahrmeijer AL, Hutteman M, van der Vorst JR, et al., 2013. Image-guided cancer surgery using near-infrared fluorescence. *Nat Rev Clin Oncol*, 10(9):507-518. https://doi.org/10.1038/nrclinonc.2013.123

Vallabhajosula S, Nikolopoulou A, Babich JW, et al., 2014. ^{99m}Tc-labeled small-molecule inhibitors of prostate-specific membrane antigen: pharmacokinetics and biodistribution studies in healthy subjects and patients with metastatic prostate cancer. *J Nucl Med*, 55(11):1791-1798. https://doi.org/10.2967/jnumed.114.140426

Vargas HA, Wassberg C, Fox JJ, et al., 2014. Bone metastases in castration-resistant prostate cancer: associations between morphologic CT patterns, glycolytic activity, and androgen receptor expression on PET and overall survival. *Radiology*, 271(1):220-229. https://doi.org/10.1148/radiol.13130625

Vargas HA, Kramer GM, Scott AM, et al., 2018. Reproducibility and repeatability of semiquantitative ^{18}F-fluorodihydrotestosterone uptake metrics in castration-resistant prostate cancer metastases: a prospective multicenter study. *J Nucl Med*, 59(10):1516-1523. https://doi.org/10.2967/jnumed.117.206490

Varnosfaderani ZG, Emamzadeh R, Nazari M, et al., 2019. Detection of a prostate cancer cell line using a bioluminescent affiprobe: an attempt to develop a new molecular probe for ex vivo studies. *Int J Biol Macromol*, 138:755-763. https://doi.org/10.1016/j.ijbiomac.2019.07.085

Vasalou C, Helmlinger G, Gomes B, 2015. A mechanistic tumor penetration model to guide antibody drug conjugate design. *PLoS ONE*, 10(3):e0118977. https://doi.org/10.1371/journal.pone.0118977

Wang GC, Hong HY, Zang J, et al., 2022. Head-to-head comparison of [^{68}Ga]Ga-P16-093 and [^{68}Ga]Ga-PSMA-617 in dynamic PET/CT evaluation of the same group of recurrent prostate cancer patients. *Eur J Nucl Med Mol Imaging*, 49(3):1052-1062. https://doi.org/10.1007/s00259-021-05539-1

Wang R, Shen GH, Huang MX, et al., 2021. The diagnostic role of ^{18}F-choline, ^{18}F-fluciclovine and ^{18}F-PSMA PET/CT in the detection of prostate cancer with biochemical recurrence: a meta-analysis. *Front Oncol*, 11:684629. https://doi.org/10.3389/fonc.2021.684629

Wang Y, de Leon AC, Perera R, et al., 2021. Molecular imaging of orthotopic prostate cancer with nanobubble ultrasound contrast agents targeted to PSMA. *Sci Rep*, 11:4726. https://doi.org/10.1038/s41598-021-84072-5

Weissleder R, Mahmood U, 2001. Molecular imaging. *Radiology*, 219(2):316-333.

https://doi.org/10.1148/radiology.219.2.r01ma19316

Wieser G, Mansi R, Grosu AL, et al., 2014. Positron emission tomography (PET) imaging of prostate cancer with a gastrin releasing peptide receptor antagonist—from mice to men. *Theranostics*, 4(4):412-419. https://doi.org/10.7150/thno.7324

Xia L, Meng XX, Wen L, et al., 2021. A highly specific multiple enhancement theranostic nanoprobe for PET/MRI/PAI image-guided radioisotope combined photothermal therapy in prostate cancer. *Small*, 17(21):2100378. https://doi.org/10.1002/smll.202100378

Yin TH, Wang K, Qiu C, et al., 2020. Simple structural indocyanine green-loaded microbubbles for dual-modality imaging and multi-synergistic photothermal therapy in prostate cancer. *Nanomed Nanotechnol Biol Med*, 28:102229. https://doi.org/10.1016/j.nano.2020.102229

You HJ, Shang WT, Min XD, et al., 2020. Sight and switch off: nerve density visualization for interventions targeting nerves in prostate cancer. *Sci Adv*, 6(6):eaax6040. https://doi.org/10.1126/sciadv.aax6040

Yu WX, Zhao M, Deng YJ, et al., 2023. Meta-analysis of ^{18}F-PSMA-1007 PET/CT, ^{18}F-FDG PET/CT, and ^{68}Ga-PSMA PET/CT in diagnostic efficacy of prostate Cancer. *Cancer Imaging*, 23(1):77. https://doi.org/10.1186/s40644-023-00599-y

Yuan M, Wu Y, Zhao CY, et al., 2022. Activated molecular probes for enzyme recognition and detection. *Theranostics*, 12(3):1459-1485. https://doi.org/10.7150/thno.66676

Zare H, Rajabibazl M, Rasooli I, et al., 2014. Production of nanobodies against prostate-specific membrane antigen (PSMA) recognizing LnCaP cells. *Int J Biol Markers*, 29(2):169-179. https://doi.org/10.5301/jbm.5000063

Zhang JL, Cheng DF, He JY, et al., 2021. Cargo loading within ferritin nanocages in preparation for tumor-targeted delivery. *Nat Protoc*, 16(10):4878-4896. https://doi.org/10.1038/s41596-021-00602-5

Zhao Y, Peng J, Yang JY, et al., 2019. Enhancing prostate-cancer-specific MRI by genetic amplified nanoparticle tumor homing. *Adv Mater*, 31(30):1900928. https://doi.org/10.1002/adma.201900928